*Journal of Applied Electrochemistry* **29**: 1255–1261, 1999.



# Electrocatalytic oxidation of methanol and formic acid on dispersed electrodes: Pt, Pt–Sn and Pt/M(upd) in poly(2-hydroxy-3-aminophenazine)

A. KELAIDOPOULOU, E. ABELIDOU and G. KOKKINIDIS*
*Aristotle University of Thessaloniki, Department of Chemistry, Laboratory of Physical Chemistry, 540 06 Thessaloniki, Greece*
*(*author for correspondence)*

Received 9 September 1998; accepted in revised form 16 March 1999

*Key words:* electrooxidation, formic acid, methanol, poly(2-hydroxy-3-aminophenazine), Pt particles, Pt–Sn codeposits, underpotential deposition

**Abstract**

Platinum particles dispersed in a poly(2-hydroxy-3-aminophenazine) film (pHAPh/Pt) provide a better catalyst than smooth Pt for the electrooxidation of methanol and formic acid in perchloric acid aqueous solutions. The catalytic activity of the Pt particles is further enhanced when Sn is codeposited in the polymer film. In the case of formic acid oxidation, the activity of Pt nanoparticles is influenced by adatoms of Tl, Pb and Bi deposited undepotential conditions. The upd-modified Pt particles are much more active than bare Pt particles. The morphology and identity of the metallic dispersion were examined by transmission electron microscopy.

## 1. Introduction

Recent developments in the preparation of micro- and nano-structured metal particles and their dispersion in porous materials have opened up the possibility of preparation of high performance electrocatalysts for technologically important reactions. A simple and efficient method of dispersing catalysts is the electrocrystallization of metals producing catalytic materials based on the properties of small clusters. Thus, effective electrocatalysts are now routinely prepared by the electrodeposition and dispersion of metal crystals or crystal aggregates in conducting polymer films, previously electrodeposited on an inert electrode [1–22]. It has been shown that such modified electrodes with Pt and Pt-based multimetallic assemblies are better catalysts than smooth platinum for the oxidation of organic fuels, that is, $CH_3OH$ [5, 7, 9, 10, 14, 15, 18], HCHO [14, 15], HCOOH [8, 14, 15, 19], $CH_3CH_2OH$ [18], $CH_2OHCH_2OH$ [21] and glucose [22].

So far, the polymers used are mainly polyaniline, polypyrrole and polythiophene. These polymers offer great advantages due to their very good conducting and mechanical properties and the good adhesion to the substrate electrode. However, it is of interest to extend such studies to other polymers which might be suitable as host materials of the catalyst microparticles.

In this paper we report the electrooxidation of methanol and formic acid on Pt and Pt–Sn dispersed in poly(2-hydroxy-3-aminophenazine), pHAPh, in aqueous acidic solutions. Furthermore, since the underpotential deposition of heavy metals (e.g., Pb, Tl, Bi) enhances the catalytic activity of smooth platinum for the oxidation of $CH_3OH$ [23–28], and particularly of HCOOH [27–32], we also include the effect of upd in this study. The aim is to investigate the influence of the particle size of the three-dimensional structured electrode on the formation of underpotential deposited layers and their influence on the kinetics of methanol and formic acid electrooxidation.

The electropolymerization of 2-hydroxy-3-aminophenazine, HAPh, on different electrodes was studied previously [33, 34]. The pHAPh is a ladder polymer with structure and properties closely related to those of poly(*o*-phenylenediamine) [35–37] and poly(*o*-aminophenol) [38–40]. It is a redox active polymer and the switching reaction (Scheme 1) occurs at around 0.1 V vs SHE. It is reported that it can respond to dissolved organic neutral and/or inorganic ionic species.

## 2. Experimental details

Glassy carbon discs and a platinum bead were used as working electrodes. Before each experiment, the disc electrodes were mechanically polished using emery paper and then electrochemically activated using preelectrolysis. The platinum bead was first pretreated by flame and then electrochemically activated. The modification of the carbon disc electrodes was performed in two steps: (a) electropolymerization of HAPh by poten-

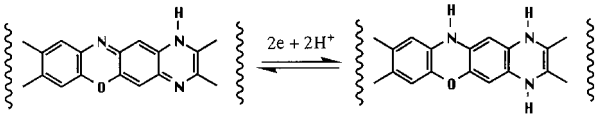


*Scheme 1.*

tial cycling ($v = 100$ mV s$^{-1}$) between $-0.15$ and $+1.65$ V vs SHE in 0.25 M $HClO_4 + 3.5 \times 10^{-4}$ M HAPh aqueous solution [33], (b) electrodeposition of platinum potentiostatically at 0.1 V vs SHE. The thickness of the polymer film was controlled by the number of potential scans (100 scans or passage of a charge of $65 \pm 5$ mC cm$^{-2}$ yielded a film of 0.3 $\mu$m). The film thickness was determined by cross-sectional views monitored with a scanning electron microscope. Further details about the film thickness are contained in [33]. The polymer film used was 0.3 $\mu$m thick, unless otherwise stated.

The solutions employed for Pt deposition and Pt–Sn, Pt–Ru codeposition were the same as in previous work [21]. The mass of the metal or metals incorporated was calculated from the charge passed considering that platinum was the only metal deposited. For the upd, the solutions of $CH_3OH$ or HCOOH contained also Tl(I), Pb(II) and Bi(III) in several concentrations ranging from $10^{-5}$ to $10^{-3}$ M. After each experiment pHAPh with the incorporated metallic particles was removed from the electrode surface by dissolution in chromic + sulfuric acid.

For the voltammetric study of methanol and formic acid, the cell used was double walled and thermostated at $25 \pm 0.1$ °C. A $Hg/Hg_2SO_4/Na_2SO_4$(sat) electrode, connected to the cell by a Luggin capillary, and a Pt sheet served as the reference and the counter electrode, respectively. The solutions were thoroughly deoxygenated by purging the cell system with ultrapure nitrogen. Electrode potentials are given on the standard hydrogen electrode (SHE) scale.

Solutions were prepared using triple distilled water and reagents from Merck ("suprapur" for $HClO_4$ and $H_2SO_4$, GR for HCl and $RuCl_3$, puriss p.a. for $CH_3OH$ and HCOOH), Fluka (puriss for $K_2PtCl_6$) and Alfa Inorganics ($NH_4[SnCl_3]$). 2-Hydroxy-3-aminophenazine was prepared from *o*-phenylenediamine and iron(III) chloride according to a known procedure [41]. Stock solutions of perchloric salts of Tl, Pb and Bi were prepared from the respective oxides or carbonates (Merck, GR grade) and perchloric acid.

The electronic set-up consisted of a home-made potentiostat, a voltage scan generator (Wenking VSG 72), a double pulse control generator (Wenking DPC 72) and a 3023 X–Y recorder from Yokogawa. For transmission electron microscopy (TEM) observations, Au (300 mesh) grids supplied by Agar Scientific Ltd were used as substrates for the polymerization of HAPh and deposition of platinum. The grids were activated by applying a continuous sweep ($v = 1$ V s$^{-1}$) between hydrogen evolution and just before oxygen evolution in 0.1 M $HClO_4$ solution until the cyclic voltammogram (0.1 V s$^{-1}$) obtained the known shape for Au. The TEM study was performed with a Joel 100CX microscope operating at 120 kV.

## 3. Results and discussion

### 3.1. *Electrooxidation of methanol*

Figure 1 shows a typical voltammogram for $CH_3OH$ electrooxidation in 0.1 M $HClO_4$ obtained with a pHAPh-modified glassy carbon electrode containing the Pt catalyst. For comparison, the voltammogram of $CH_3OH$ at a GC/Pt electrode with the same amount of deposited Pt (0.12 mg cm$^{-2}$) is also given. As on smooth platinum, the oxidation starts at around 0.5 V vs SHE and the maximum current density appears at ~0.85 V (positive sweep). The maximum current density is ~12 mA cm$^{-2}$ for GC/Pt and ~30 mA cm$^{-2}$ for GC/pHAPh/Pt. The current densities were calculated considering as electrode surface the geometric surface area of the supporting electrode. The maximum current density on smooth Pt under the same conditions is ~5.0 mA cm$^{-2}$.

The present results clearly show that the pHAPh/Pt electrode yields much higher currents than smooth Pt and platinized GC. This may be attributed, on the one hand, to the large surface area of the Pt particles and, on the other hand, to the fact that Pt micro- and nanoparticles are probably less sensitive to poisoning from adsorbed CO species. The current density of $CH_3OH$ oxidation depends on the amount of deposited Pt. For the peak that appears in the positive going sweep, the variation of the peak current density with the Pt loading is given in the inset of Figure 1. The $j_p$ increases with the mass of the metal incorporated and reaches a maximum value of about 67 mA cm$^{-2}$ at Pt loading of 0.48 mg cm$^{-2}$. Thereafter, the extra platinum added does not increase the active electrode surface area but the catalyst undergoes probably a lower degree of dispersion.

Comparing the $j_p$ vs Pt loading (inset of Figure 1) with the corresponding plot given in [14] for a polyaniline-modified glassy carbon electrode, there are two main differences. First, the maximum value of $j_p \approx 67$ mA cm$^{-2}$ observed for the GC/pHAPh/Pt electrode is much greater than the value of $j_p \approx 12$ mA cm$^{-2}$ reported for the GC/PAni/Pt electrode and, secondly, the peak current density reaches the maximum value on PAni/Pt at significantly lower Pt loading (0.07 mg cm$^{-2}$) than on pHAPh/Pt. These remarkable differences may be ascribed, on the one hand, to the fact that in the study on PAni/Pt the film was thicker (0.5 $\mu$m) and, on the other hand, to the low potential sweep rate employed (5 mV s$^{-1}$). Indeed, studies using microparticulate electrodes have shown that the catalytic activity of such electrodes is a function not only of the amount of electrodeposited catalyst but also depends on other factors, for example, the size of particles

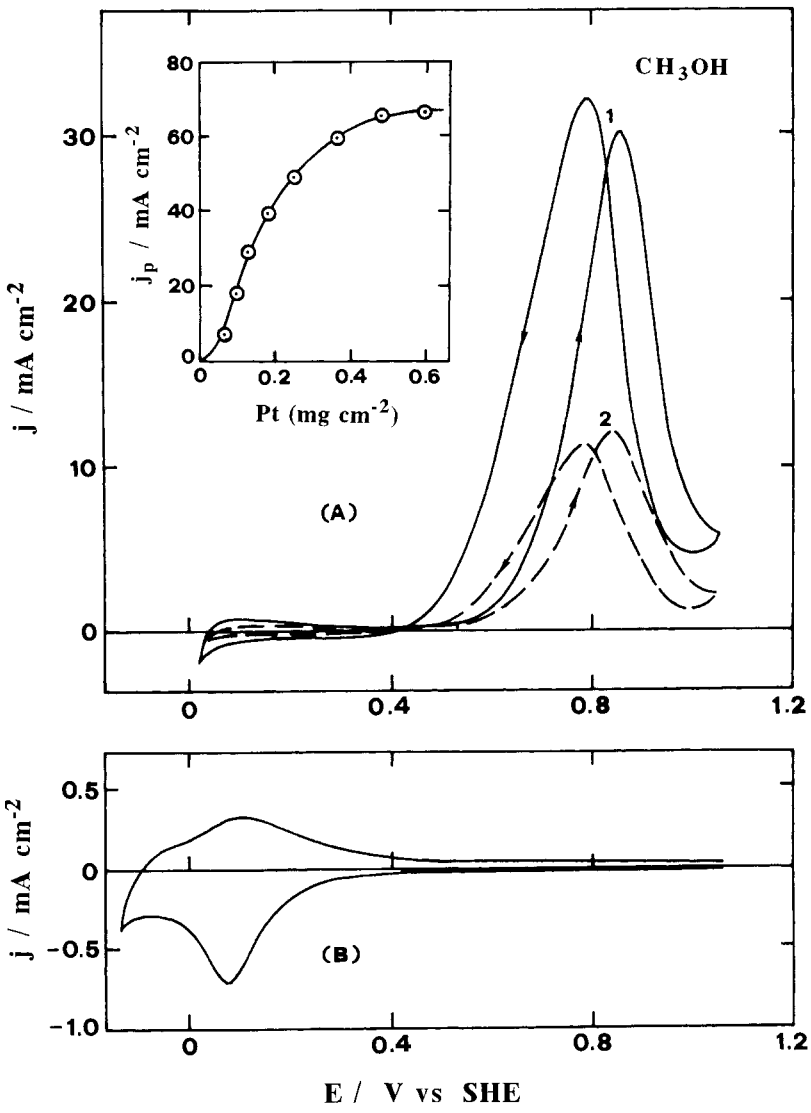


*Fig. 1.* (A) Voltammograms for $CH_3OH$ (0.1 M) oxidation obtained on (1) GC/pHAPh (0.16 $\mu$m)/Pt (0.12 mg cm$^{-2}$) and (2) GC/Pt (0.12 mg cm$^{-2}$) electrodes in 0.1 M $HClO_4$. $|dE/dt| = 50$ mV s$^{-1}$. The inset shows the plot of $j_p$ vs Pt loading for the GC/pHAPh/Pt electrode. (B) Voltammogram of the GC/pHAPh (0.16 $\mu$m) electrode in 0.1 M $HClO_4$ at $v = 50$ mV s$^{-1}$.

and the transport conditions outside and inside the film.

Therefore, in order to compare the activity of the Pt particles electrodeposited in pHAPh and PAni films, cyclic voltammograms for the oxidation of methanol on pHAPh/Pt and PAni/Pt were recorded for the same film thickness and deposition conditions, as well as the same potential sweep rate. Figure 2 shows the voltammograms for films of 0.3 $\mu$m thickness containing 0.12 mg cm$^{-2}$ Pt recorded at 5 mV s$^{-1}$. The peak current density on GC/PAni/Pt is 13 mA cm$^{-2}$ which is comparable to that previously reported [14], while on GC/pHAPh/Pt it is almost twice than that of GC/PAni/Pt, indicating higher catalytic activity for the Pt particles incorporated and dispersed in the pHAPh polymer matrix.

The morphology of the platinum particles deposited in the pHAPh and PAni films was examined by transmission electron microscopy. Figure 3 shows the TEM micrographs of pHAPh/Pt and PAni/Pt assemblies prepared under similar electrodeposition conditions. As can be seen, platinum is dispersed in pHAPh and PAni. The rings show the corresponding diffraction patterns of the platinum [21] particles. The order of magnitude of the mean diameter of the metallic particles is much smaller than one micrometre. However, in the case of PAni the nanoparticles aggregate in larger groups and this probably leads to a lower degree of dispersion. Thus, the same metallic mass leads to a smaller electrode surface area and might explain the lower catalytic activity of platinum particles dispersed in polyaniline.

In the case of pHAPh, the deposition of platinum yields spherical catalyst particles 40–70 nm in diameter. The nano-particles surround the pHAPh fibrils in a fairly uniform manner. Since the catalyst particles are dispersed throughout the polymer, penetration and diffusion of methanol through the film should be a slow process and should affect the whole mechanism. Under

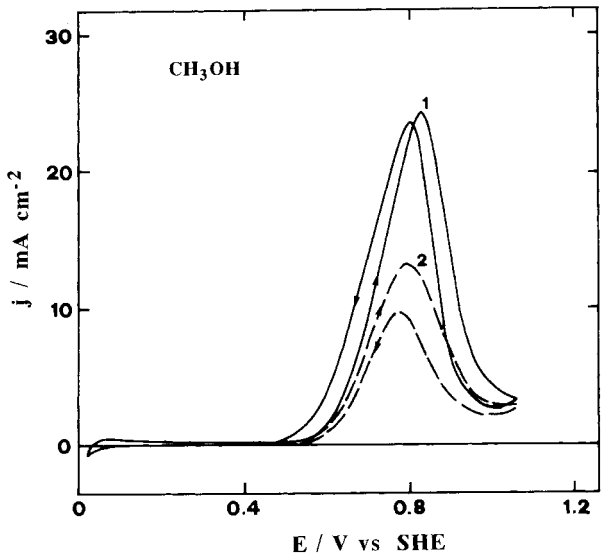


*Fig. 2.* Voltammograms for $CH_3OH$ (0.1 M) oxidation obtained on (1) GC/pHAPh (0.3 $\mu$m)/Pt (0.12 mg cm$^{-2}$) and (2) GC/PAni (0.3 $\mu$m)/Pt (0.12 mg cm$^{-2}$) electrodes in 0.1 M $HClO_4$. $|dE/dt| = 5$ mV s$^{-1}$.

rotating conditions and for low rotation rates the height of the current peaks increases with the rotation rate in such a manner that the $j^{-1}$ vs $\omega^{-1/2}$ dependence (Koutecky–Levich analysis) gives straight lines. The intercept of the $j_p^{-1}$ vs $\omega^{-1/2}$ plots is proportional to the film thickness, indicating that transport of $CH_3OH$ through the film is, indeed, one of the controlling factors. This behaviour verifies that the platinum particles are not concentrated on the polymer–solution interface but dispersed in a three-dimensional manner in the polymer matrix. Similar behaviour was also observed with PAni/Pt electrodes in the case of $CH_3OH$ [5] and ethylene glycol [21] oxidation.

Previous studies concerning the oxidation of $CH_3OH$ [7, 15, 18] and other organic fuels [18, 19, 21] have shown that the catalytic activity of dispersed electrodes is even more enhanced when, instead of Pt alone, Pt–Sn and Pt–Ru catalyst systems are employed. The results for the oxidation of methanol on platinum supported catalysts show trends that are similar to methanol oxidation on Pt electrodes modified with Sn and Ru ad-atoms [42–44].

For the incorporation of the binary catalyst particles into the pHAPh matrix, we followed the same procedure described previously for polyaniline [21] (see also Section 2). With this method only Sn was codeposited with Pt in the pHAPh film, while (in contrast to polyaniline) Ru was not deposited. The codeposited Pt–Sn particles are similar in size (40–70 nm in diameter) to that of Pt particles alone. However, the only phase detected by transmission electron microscopy was Pt since no Sn rings were observed in the corresponding diffraction patterns. A reasonable explanation could be that Sn exists in the form of ad-atoms on Pt nanocrystallites or that the condensed mass of Sn crystallites is too low to be detected. X-ray analysis of the pHAPh/Pt–Sn assembly has shown that the amount of Sn is around 1%. In the case of codeposition of Ru with Pt the X-ray analysis of the corresponding samples have shown that Ru does not exist either as non-oxidized or oxidized particles in the pHAPh/Pt assembly.

Figure 4 shows the cyclic voltammograms for the oxidation of $CH_3OH$ on pHAPh-modified glassy carbon electrodes containing the Pt and Pt–Sn catalyst particles.

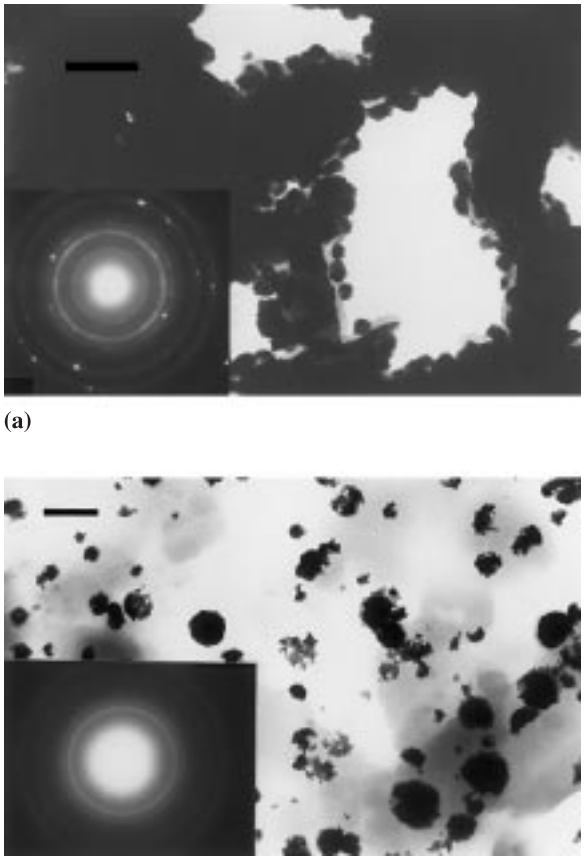


*Fig. 3.* TEM images of (a) pHAPh/Pt and (b) PAni/Pt electrodes and the corresponding diffraction patterns (bar $\equiv$ 0.2 $\mu$m for both micrographs).

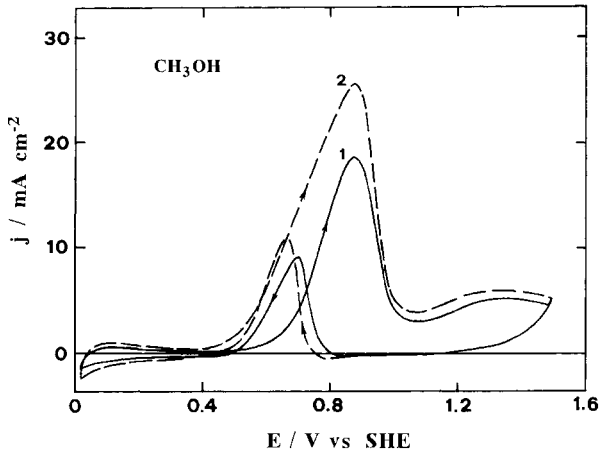


*Fig. 4.* Voltammograms for $CH_3OH$ (0.1 M) oxidation obtained on (1) GC/pHAPh (0.3 $\mu$m)/Pt (0.1 mg cm$^{-2}$) and (2) GC/pHAPh (0.3 $\mu$m)/Pt–Sn (0.1 mg cm$^{-2}$) electrodes in 0.1 M $HClO_4$. $|dE/dt| = 50$ mV s$^{-1}$.

The onset of current for methanol oxidation on the pHAPh/Pt–Sn assembly occurs at less positive potential (~130 mV) and higher currents are obtained, indicating an enhanced electrocatalytic activity in the whole potential range compared with pure dispersed platinum. The currents recorded during the positive and negative sweeps are very close to each other, which is an indication of weaker poisoning effect [15]. Earlier studies on bimetallic assemblies [15, 16, 45–49] have shown that the oxygen species, which are necessary for the oxidation of organic fuels on platinum, start to form at lower potentials on Sn sites and readily react with the carbon adsorbed species on Pt sites. This bifunctional mechanism should be responsible for the decrease in the overpotential of $CH_3OH$ electrooxidation observed in the case of the pHAPh/Pt–Sn assembly.

The influence of Pb ad-atoms deposited at underpotential conditions on the oxidation of $CH_3OH$ on Pt nanoparticles was also studied. According to the literature [25, 26], smooth platinum modified by underpotential monolayers of Pb is a slightly better catalyst than pure Pt towards methanol electrooxidation in acid solutions. However, the underpotential deposition of Pb on Pt nanoparticles dispersed in pHAPh had almost no effect for $CH_3OH$ oxidation.

### 3.2. *Electrooxidation of formic acid*

Figure 5 shows voltammograms corresponding to the oxidation of formic acid on smooth platinum and Pt (0.1 mg $cm^{-2}$) electrodeposited on GC and GC/pHAPh electrodes. The shape of the voltammograms is the same for all electrodes differing only in the strength of the current densities. For GC/Pt and GC/pHAPh/Pt, the current densities were calculated considering as electrode surface the geometric surface area of the GC electrode.

As can be seen, the highest currents are obtained with the GC/pHAPh/Pt electrode. This is mainly attributable to the large surface area of the Pt particles dispersed in the pHAPh polymer matrix. The nature of the pHAPh/Pt assembly was described above. Despite the large surface area of Pt dispersed in pHAPh, the currents on the GC/pHAPh/Pt electrode still remain very low at potentials negative of 0.65 V indicating that poisoning from adsorbed CO species is also significant for formic acid oxidation on the Pt nano-particles.

The deposition of Pt–Sn might offer better catalysts for formic acid oxidation. A substantial difference between the pHAPh supported Pt–Sn and Pt catalyst can be seen in their activity for HCOOH oxidation. Figure 6 compares the activity of a pHAPh/Pt–Sn and a pHAPh/Pt assembly for HCOOH oxidation. The significant result shown in Figure 6 is that the Pt–Sn catalyst has higher activity at potentials negative of 0.65 V and that the Pt activity is somewhat better at more positive potentials. This behaviour clearly shows that the poisoning effect is markedly decreased by the presence of Sn, which is in agreement with results described previously [16] for the Pt–Sn catalyst dispersed in polyaniline.

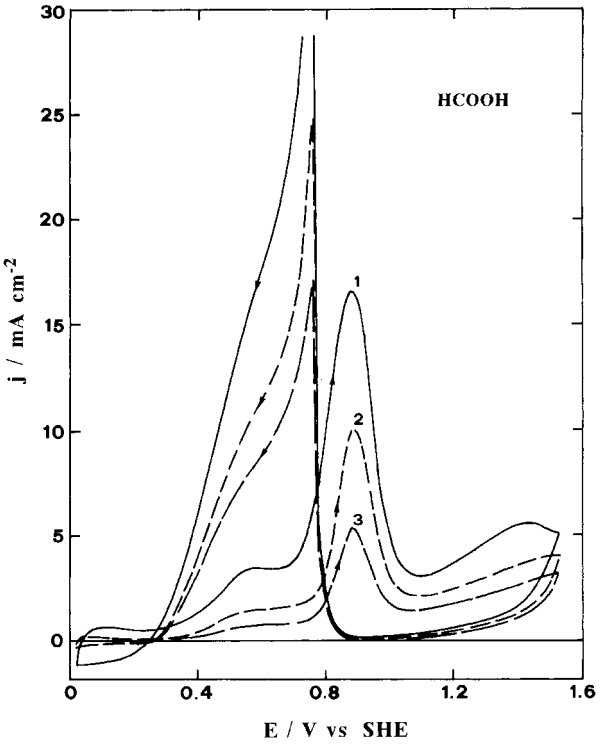


*Fig. 5.* Voltammograms for HCOOH (0.1 M) oxidation obtained on (1) GC/pHAPh (0.3 $\mu$m)/Pt (0.1 mg $cm^{-2}$), (2) GC/Pt (0.1 mg $cm^{-2}$) and (3) Pt bead, electrodes in 0.1 M $HClO_4$. $|dE/dt| = 50$ mV $s^{-1}$.

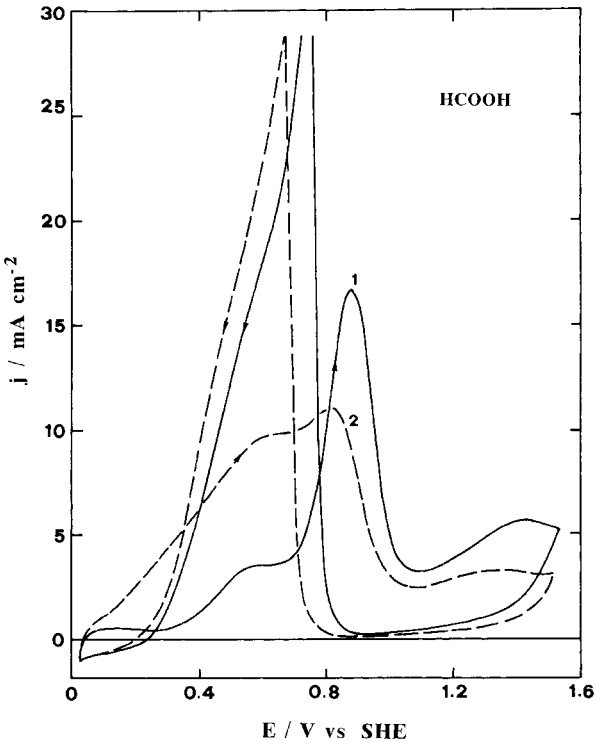


*Fig. 6.* Voltammograms for HCOOH (0.1 M) oxidation obtained on (1) GC/pHAPh (0.3 $\mu$m)/Pt (0.1 mg $cm^{-2}$) and (2) GC/pHAPh (0.3 $\mu$m)/Pt–Sn (0.1 mg $cm^{-2}$) electrodes in 0.1 M $HClO_4$. $|dE/dt| = 50$ mV $s^{-1}$.

It is well known [27–32] that the oxidation of formic acid on smooth Pt is strongly enhanced by ad-atoms of heavy metals deposited at underpotential conditions. Like smooth Pt, the catalytic activity of Pt nanoparticles dispersed in pHAPh is substantially enhanced by the underpotential deposition of heavy metals. Figure 7 shows the voltammograms of the electrooxidation of HCOOH on the GC/pHAPh/Pt electrodes modified by underpotential deposited layers of Tl, Pb and Bi. The voltammograms represent the first scan, but the second and the following scans display the same shape.

As can be seen, the Tl and Pb ad-atoms cause a positive catalytic effect both in terms of potential and current density. The onset of oxidation is shifted towards less positive potentials (~200 mV) and much higher currents are obtained at potentials negative of 0.7 V. With Bi ad-atoms catalysis is observed only in terms of the current density. In the experiments with Bi(upd) the negative potential limit was kept below 0.2 V to avoid bulk deposition of bismuth. Maximum catalytic activity was obtained with concentrations of heavy metal ions in solution $5 \times 10^{-4}$ M for $Pb^{2+}$ and $10^{-4}$ M for $Tl^{+}$ and $Bi^{3+}$.

The data for the influence of upd on formic acid oxidation on the pHAPh/Pt electrodes are comparable with those previously described [29, 30] for smooth platinum. Like smooth Pt, the electrocatalytic activity of the upd-modified Pt particles can be explained by considering that the ad-atoms prevent poison formation according the the well known [27, 28] 'third body' mechanism.

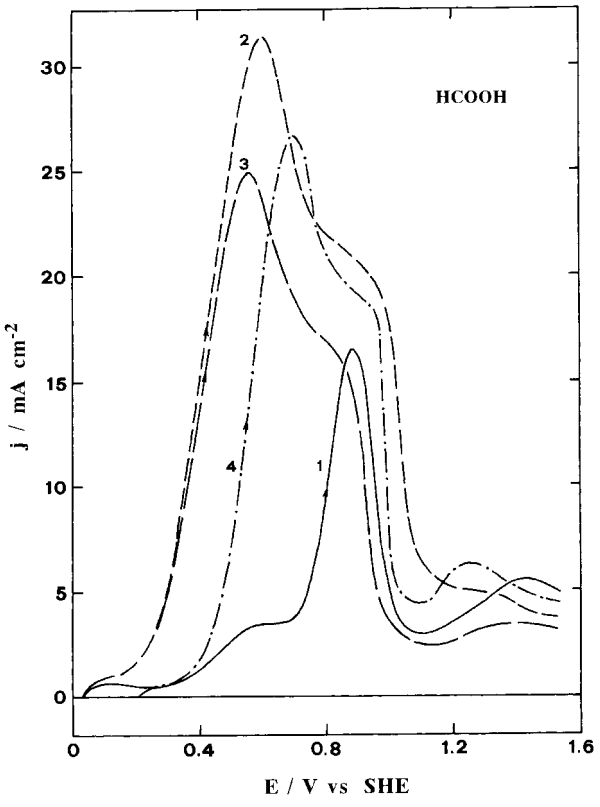


*Fig. 7.* Voltammograms for HCOOH (0.1 M) oxidation obtained on GC/pHAPh (0.3 $\mu$m)/Pt (0.1 mg cm$^{-2}$) electrodes in the absence (1) and presence of (2) $10^{-4}$ M $TlClO_4$, (3) $5 \times 10^{-4}$ M $Pb(ClO_4)_2$ and (4) $10^{-4}$ M $Bi(ClO_4)_3$ in 0.1 M $HClO_4$. $|dE/dt| = 50$ mV s$^{-1}$.

## 4. Conclusions

We have studied electrodes modified with poly(2-hydroxy-3-aminophenazine) and Pt, Pt–Sn and Pt/M(upd) particles. Platinum dispersed in pHAPh is a much better catalyst than smooth Pt for the electrooxidation of methanol and formic acid in aqueous perchloric acid solutions. The catalytic activity of the Pt particles is further enhanced when Sn is codeposited in the polymer film. TEM observations have shown that the deposition of platinum yields spherical catalyst particles (40–70 nm in diameter) which are homogeneously distributed in the pHAPh matrix. The Pt–Sn particles are similar in size to that of Pt particles alone. The amount of Sn deposited is around 1%.

In the case of formic acid electrooxidation, the activity of the Pt nano-particles is influenced by modification with ad-atoms of Tl, Pb and Bi deposited in the underpotential region. The upd-modified Pt particles are much more active than the bare Pt particles. The Pt particles are sensitive to poison formation and the upd ad-atoms improve their activity by minimizing the poisoning reaction. It is likely that the particle size of the nanostructured material influences the kinetics of formic acid oxidation. However, in order to draw any concrete conclusion on this matter and on the effect of upd, the influence of the particle size on the formation of underpotential deposited layers and their influence on the oxidation of formic acid should be studied more systematically.

## Acknowledgement

This work was performed within a research project (PENED Oct. 1996, code 1706) supported by the General Secretary of Research and Technology, Greece.

## References

1. G. Tourillon and F. Garnier, *J. Phys. Chem.* **88** (1984) 5281.
2. W.-H. Kao and T. Kuwana, *J. Am. Chem. Soc.* **106** (1984) 473.
3. D.E. Bartak, B. Kazee, K. Shimazu and T. Kuwana, *Anal. Chem.* **58** (1986) 2756.
4. L. Coche and J.-C. Moutet, *J. Am. Chem. Soc.* **109** (1987) 6887.
5. K.M. Kost, D.E. Bartak, B. Kazee and T. Kuwana, *Anal. Chem.* **60** (1988) 2379.
6. S. Holdcroft and B.L. Funt, *J. Electroanal. Chem.* **240** (1988) 89.
7. P.O. Esteban, J.-M. Léger, C. Lamy and E. Genies, *J. Appl. Electrochem.* **19** (1989) 462.
8. M. Gholamian and A.Q. Contractor, *J. Electroanal. Chem.* **289** (1990) 69.
9. D.J. Strike, N.F. De Rooij, M. Koudelka-Hep, M. Ulmann and J. Augustynski, *J. Appl. Electrochem.* **22** (1992) 922.
10. M. Ulmann, R. Kostecki, J. Augustynski, D.J. Strike and M. Koudelka-Hep, *Chimia* **46** (1992) 138.

11. A. Leone, W. Marino and B.R. Scharifker, *J. Electrochem. Soc.* **139** (1992) 438.
12. C.S.C. Bose and K. Rajeshwar, *J. Electroanal. Chem.* **333** (1992) 235.
13. C.C. Chen, C.S.C. Bose and K. Rajeshwar, *J. Electroanal. Chem.* **350** (1993) 161.
14. H. Laborde, J.-M. Léger and C. Lamy, *J. Appl. Electrochem.* **24** (1994) 219.
15. W.T. Napporn, H. Laborde, J.-M. Léger and C. Lamy, *J. Electroanal. Chem.* **404** (1996) 153.
16. W.T. Napporn, J.-M. Léger and C. Lamy, *J. Electroanal. Chem.* **408** (1996) 141.
17. S. Ye, A.K. Vijh and L.H. Dao, *J. Electroanal. Chem.* **415** (1996) 115.
18. C.T. Hable and M.S. Wrighton, *Langmuir* **9** (1993) 3284.
19. R. Schrebler, M.A. del Valle, H. Gomez, C. Veas and R. Cordova, *J. Electroanal. Chem.* **380** (1995) 219.
20. Y. Takasu, N. Ohashi, X.-G. Zhang, Y. Murakami, H. Minagawa, S. Sato and K. Yahikozawa, *Electrochim. Acta* **41** (1996) 2595.
21. A. Kelaidopoulou, E. Abelidou, A. Papoutsis, E.K. Polychroniadis and G. Kokkinidis, *J. Appl. Electrochem.* **28** (1998) 1101.
22. A. Kelaidopoulou, A. Papoutsis, G. Kokkinidis, W.T. Napporn, J.-M. Léger and C. Lamy, *J. Appl. Electrochem.* **29** (1999) 101.
23. S. Motoo and M. Watanabe, *J. Electroanal. Chem.* **60** (1975) 259.
24. Yu. B. Vassiliev, V.S. Bagotzky, N.V. Osetrova and A.A. Mikhailova, *J. Electroanal. Chem.* **97** (1979) 63.
25. B. Beden, F. Kadirgan, C. Lamy and J.-M. Léger, *J. Electroanal. Chem.* **127** (1981) 75; **142** (1982) 171.
26. G. Kokkinidis and D. Jannakoudakis, *J. Electroanal. Chem.* **153** (1983) 185.
27. R.R. Adzic, in H. Gerischer and C.W. Tobias (Eds.), 'Advances in Electrochemistry and Electrochemical Engineering', Vol. 13 (J. Wiley & Sons, New York, 1984), p. 159.
28. G. Kokkinidis, *J. Electroanal. Chem.* **201** (1986) 206.
29. R.R. Adzic, D.N. Simic, A.R. Despic and D.M. Drazic, *J. Electroanal. Chem.* **61** (1975) 117; **65** (1975) 587.
30. R.R. Adzic, D.N. Simic, A.R. Despic and D.M. Drazic, *J. Electroanal. Chem.* **80** (1977) 81.
31. S. Motoo and M. Watanabe, *J. Electroanal. Chem.* **98** (1979) 203.
32. I. Fonseca, J. Lin Cai and D. Pletcher, *J. Electrochem. Soc.* **130** (1983) 2187.
33. G. Kokkinidis, A. Papoutsis and I. Poulios, *J. Electroanal. Chem.* **379** (1994) 379.
34. A. Kelaidopoulou, A. Papoustis, G. Kokkinidis and E.K. Polychroniadis, *J. Electroanal. Chem.* **404** (1996) 113.
35. K. Chiba, T. Ohsaka, Y. Ohnuki and N. Oyama, *J. Electroanal. Chem.* **219** (1987) 117.
36. J. Yano, A. Shimoyama and K. Ogura, *J. Chem. Soc. Faraday Trans.* **88** (1992) 2523.
37. D. Sazou, I. Poulios and G. Kokkinidis, *Synth. Met.* **32** (1989) 113.
38. T. Ohsaka, S. Kunimura and N. Oyama, *Electrochim. Acta* **33** (1988) 639.
39. S. Kunimura, T. Ohsaka and N. Oyama, *Macromolecules* **21** (1988) 894.
40. C. Barbero, J.J. Silber and L. Sereno, *J. Electroanal. Chem.* **263** (1989) 333.
41. F. Ulman and F. Mauthner, *Chem. Ber.* **35** (1902) 4302.
42. H.A. Gasteiger, N.M. Markovic, P.N. Ross Jr and E.J. Cairns, *Electrochim. Acta* **39** (1994) 1825.
43. N.M. Markovic, H.A. Gasteiger, P.N. Ross Jr, X. Jiang, I. Villegas and M.J. Weaver, *Electrochim. Acta* **40** (1995) 91.
44. W. Chrzanowski and A. Wieckowski, *Langmuir* **14** (1998) 1967.
45. S. Motoo and M. Watanabe, *J. Electroanal. Chem.* **69** (1976) 429.
46. M. Shibata and S. Motoo, *J. Electroanal. Chem.* **229** (1987) 385.
47. S. Swathirajan and Y.M. Mikhail, *J. Electrochem. Soc.* **139** (1992) 2105.
48. M. Krausa and W. Vielstich, *J. Electroanal. Chem.* **379** (1994) 307.
49. H.A. Gasteiger, N.M. Markovic and P.N. Ross Jr, *J. Phys. Chem.* **99** (1995) 8945.